2248 *Chem. Mater.* **2010,** *22,* 2248–2254
DOI:10.1021/cm903024h

CHEMISTRY OF MATERIALS
Article

Self-Limiting Robust Surface-Grafted Organic Nanofilms

L. Todd Banner,[†,‡] Samuel Tekobo,[†,‡] Fernando Garay,[†,§] Benjamin T. Clayton,[†,‡] Zachary P. Thomas,[†,‡] Ernö Lindner,[†,§] Andrew G. Richter,[⊥] and Eugene Pinkhassik*[,†,‡]

[†]*Institute for Nanomaterials Development and Innovation at the University of Memphis (INDIUM),* [‡]*Department of Chemistry, and* [§]*Department of Biomedical Engineering, University of Memphis, Memphis, Tennessee 38152, and* [⊥]*Department of Physics and Astronomy, Valparaiso University, Valparaiso, Indiana 46383*

Received September 29, 2009. Revised Manuscript Received February 19, 2010

Robust surface-bound insulating polymer films with controlled thickness in < 5 nm range are important for technological advances in diverse disciplines such as electrochemical sensors, molecular electronics, separations, and anticorrosive coatings. Creating these films by simple methods from readily available materials has been a significant challenge. Here we report a newly synthesized molecule combining styrene and thiol moieties, joined via a short linker, that binds to the gold surface, polymerizes, and cross-links polymer chains to form robust films with uniform and controlled thickness and complete surface coverage. Additional layers can be deposited. These films that bridge two- and three-dimensional materials show excellent stability and insulating properties.

Introduction

Coating of surfaces with covalently bound, insulating polymer films of precisely controlled thicknesses in the 1−5 nm range is an elusive goal of nanomaterials research. Nanothin coatings on the surfaces of electrochemical sensors offer unique advantages for minimizing background noise while inducing or enhancing selectivity toward certain analytes.[1] Molecular imprinting of analytes may result in better uniformity of recognition sites than in bulk polymers and better three-dimensional control compared with two-dimensional monolayers.[2] In addition, covalently bound nanothin films are paramount in the progress of a variety of interdisciplinary research fields including molecular electronics,[3] separations,[4] biosensors,[5] and anticorrosive coatings.[6] Although there are numerous reports on self-assembled monolayers (SAM),[7] SAM-based polymer grafts,[8] brushes,[9] and spin-coated polymers,[10] cross-linked insulating surface-mounted films with < 5 nm thickness prepared by simple methods are rare.

Here we describe the synthesis and characterization of nanofilms formed from a newly synthesized compound **1** that binds to the surface, polymerizes, and cross-links its polymer chains to form robust and insulating films with controlled and uniform thickness (Figure 1).

We designed a molecule combining a styrene moiety, which can be easily polymerized, with a thiol group attached via a short linker. The thiol group plays a dual role: it binds strongly to the gold surface[11] and copolymerizes with the styrene moiety via thiol−ene chemistry (Figure 2).[12] Because **1** has two reactive groups, it can also cross-link the chains, making the films robust and enabling the film growth in three dimensions.

Experimental Section

3-Bromopropylbenzene was purchased from Alfa-Aesar. Acetic anhydride and hydrogen peroxide were purchased from Fisher Scientific. All other chemicals were purchased from Sigma-Aldrich and used without further purification. Thin layer chromatography (TLC) was performed with silica G TLC plates with UV254 aluminum backed, 200 μm purchased from Sorbent Technologies. Flash chromatography was performed with an Analogix pump and Analogix Superflash silica columns purchased from Sorbent Technologies. Semipreparative HPLC (high-performance liquid chromatography) was performed with

*Corresponding author. E-mail: epnkhssk@memphis.edu.

(1) Sallacan, N.; Zayats, M.; Bourenko, T.; Kharitonov, A. B.; Willner, I. *Anal. Chem.* **2002**, *74*, 702–712.
(2) (a) Huan, S.; Shen, G.; Yu, R. *Electroanalysis* **2004**, *16*, 1019–1023. (b) Menaker, A.; Syritski, V.; Reut, J.; Öpik, A.; Horváth, V.; Gyurcsányi, R. E. *Adv. Mater.* **2009**, *21*, 2271–2275.
(3) Zhou, C.; Nagy, G.; Walker, A. V. *J. Am. Chem. Soc.* **2005**, *127*, 12160–12161.
(4) (a) Wulff, G. *Chem. Rev.* **2002**, *102*, 1–28. (b) Sellergren, B. *J. Chromatogr., A* **2001**, *906*, 227–252.
(5) Cosnier, S. *Biosens. Bioelectron.* **1999**, *14*, 443–456.
(6) Hamdy, A. S. *Mater. Lett.* **2006**, *60*, 2633–2637.
(7) Love, J. C.; Estroff, L. A.; Kriebel, J. K.; Nuzzo, R. G.; Whitesides, G. M. *Chem. Rev.* **2005**, *105*, 1103–1169.
(8) (a) Harant, A. W.; Khire, V. S.; Thibodaux, M. S.; Bowmann, C. N. *Macromolecules* **2006**, *39*, 1461–1466. (b) Khire, V. S.; Harant, A. W.; Watkins, A. W.; Anseth, K. S.; Bowman, C. N. *Macromolecules* **2006**, *39*, 5081–5086.
(9) Ducker, R.; Garcia, A.; Zhang, J. M.; Chen, T.; Zauscher, S. *Soft Matter* **2008**, *4*, 1774–1786.
(10) Weill, A.; Dechenaux, E. *Polym. Eng. Sci.* **1998**, *28*, 945–948.
(11) Nuzzo, R. G.; Zegarski, B. R.; Dubois, L. H. *J. Am. Chem. Soc.* **1987**, *109*, 733–740.
(12) (a) Cramer, N. B.; Davies, T.; O'Brien, A. K.; Bowman, C. N. *Macromolecules* **2003**, *36*, 4631–4636. (b) Senyurt, A. F.; Wei, H.; Phillips, B.; Cole, M.; Nazarenko, S.; Hoyle, C. E.; Piland, S. G.; Gould, T. E. *Macromolecules* **2006**, *39*, 6315–6317. (c) Cramer, N. B.; Reddy, S. K.; Cole, M.; Hoyle, C.; Bowman, C. N. *J. Polym. Sci., A: Polym. Chem.* **2004**, *42*, 5817. (d) Cramer, N. B.; Scott, J. P.; Bowmann, C. N. *Macromolecules* **2002**, *35*, 5361–5365.

 Published on Web 03/11/2010

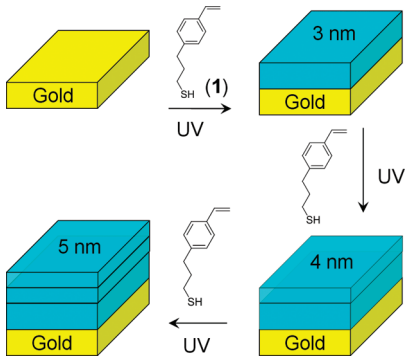

Figure 1. Schematic representation of controlled film formation and sequential layer depositions from **1**.

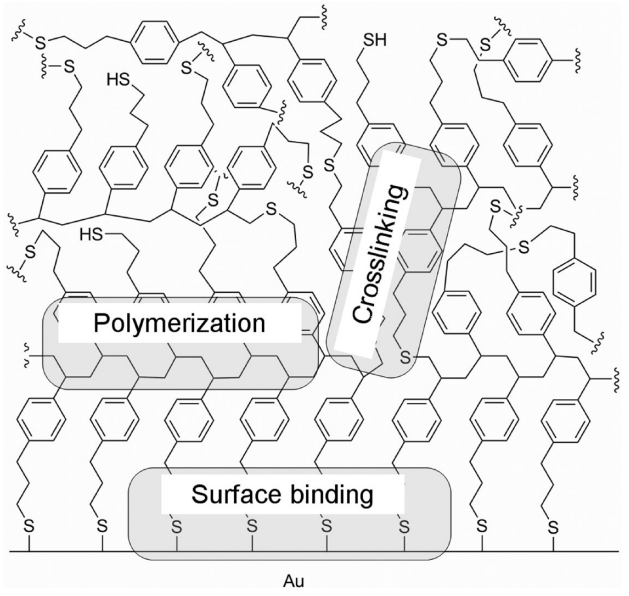

Figure 2. Plausible film structure highlighting the triple function of **1**.

a Waters 600 pump and Waters 2487 detector equipped with a semiprep flow cell. The detection wavelength was 255 nm. The column was a Nova-Pak Silica, 6 μm, 19 × 300 mm. The flow rate was 10 mL/min. Elemental analyses were performed by Desert Analytics (Tucson, Arizona). Gas chromatography with electron impact ionization and mass spectrometry was performed with a Hewlett-Packard G1800A GCD System using a ValcoBond VB-5 capillary column (30 m × 0.25 mm × 25 μm) and a temperature gradient from 80 to 300 °C.

Synthesis of 1-(4-(3-Bromopropyl)phenyl)ethanone (3). $AlCl_3$ (15.0 g, 110 mmol) was added to CH_2Cl_2 (100 mL) under an inert atmosphere. The reaction flask was cooled in an ice bath. Acetic anhydride (5.6 g, 55 mmol) diluted with CH_2Cl_2 (5 mL) was then added over 30 min. The mixture was stirred for an additional 15 min. **2** (5.0 g, 25 mmol) was diluted with CH_2Cl_2 (5 mL) and was added to the reaction mixture over 30 min. The mixture was stirred for an additional 2 h while being cooled in an ice bath. The mixture was slowly poured onto 200 g of crushed ice. The organic phase was washed with 10% HCl (3 × 50 mL), saturated $NaHCO_3$ (3 × 50 mL), and saturated NaCl (3 × 50 mL). The solvent was removed under a vacuum, and crude product was purified by flash chromatography using CH_2Cl_2 (R_f = 0.99 by TLC) and then by semipreparative HPLC using 75% hexane/25% ethyl acetate to give **3** as a liquid (yield 55%). ^{1}H NMR (270 MHz, $CDCl_3$): δ 7.88 (d, 2 H, J = 8.2 Hz), 7.26 (d, 2 H, J = 8.2 Hz), 3.37 (t, 2 H, J = 6.4 Hz), 2.83 (t, 2 H, J = 7.4 Hz), 2.57 (s, 3 H), 2.22 - 2.11 (m, 2 H). ^{13}C NMR (67.5 MHz, $CDCl_3$): 197.66, 128.84, 128.74, 146.36, 135.51, 34.03, 33.74, 32.74, and 26.62 ppm. Elem. anal. Calcd for $C_{11}H_{13}BrO$: C, 54.79; H, 5.43. Found: C, 54.88; H, 5.24.

Synthesis of 1-(4-(3-Bromopropyl)phenyl)ethanol (4). 3 (4.624 g, 19 mmol) was diluted with methanol (60 mL) in a reaction flask under an inert atmosphere. The reaction flask was cooled in an ice bath. $NaBH_4$ (0.75 g, 20 mmol) was added to the mixture over 5 min. The mixture was stirred for an additional 2 h. Saturated NaCl (70 mL) was added to the mixture and the product was extracted with CH_2Cl_2 (2 × 20 mL). The organic phase was washed with saturated NaCl (3 × 50 mL). The solvent was removed under a vacuum to recover the crude product, which was purified by flash chromatography using 50% hexane/50% ethyl acetate (R_f = 0.68 by TLC) and then by semi-preparative HPLC using 60% hexane/40% ethyl acetate to give **4** as a colorless liquid (yield 60%). ^{1}H NMR (270 MHz, $CDCl_3$): δ 7.29 (d, 2 H, J = 8.2 Hz), 7.17 (d, 2 H, J = 8.2 Hz), 4.87−4.85 (m, 1 H), 3.38 (t, 2 H, J = 6.6 Hz), 2.76 (t, 2 H, J = 7.4 Hz), 2.20−2.10 (m, 2 H), 1.86−1.85 (m, 1 H), 1.49−1.46 (m, 3 H). ^{13}C NMR (270 MHz, $CDCl_3$): 143.79, 139.87, 128.76, 125.69, 70.26, 34.22, 33.69, 33.13, and 25.18 ppm. Elem. anal. Calcd for $C_{11}H_{15}BrO$: C, 54.34; H, 6.22. Found: C, 54.59; H, 6.28.

Synthesis of 1-(3-Bromopropyl)-4-vinylbenzene (5). 4 (3.169 g, 13 mmol) and *p*-toluenesulfonic acid (0.125 g, 0.7 mmol) were dissolved in toluene (200 mL). The reaction mixture was refluxed for 3 h in an inert atmosphere, and water was removed with a Dean−Stark collector. The mixture was washed with water (3 × 50 mL), the solvent was removed under a vacuum, and crude product was purified by flash chromatography using 90% hexane/10% ethyl acetate (R_f = 0.75 by TLC) and then semipreparative HPLC using 99% hexane and 1% ethyl acetate to give 5 as a colorless liquid (yield 47%). ^{1}H NMR (270 MHz, $CDCl_3$): δ 7.36 (d, 2 H, J = 8.2 Hz), 7.17 (d, 2 H, J = 8.2 Hz), 6.71 (q, 1 H), 5.76−5.70 (m, 1 H), 5.24 − 5.20 (m, 1 H), 3.40 (t, 2 H, J = 6.7 Hz), 2.78 (t, 2 H, J = 7.2 Hz), 2.19−2.14 (m, 2 H). ^{13}C NMR (270 MHz, $CDCl_3$): 140.33, 136.66, 135.74, 128.84, 126.47, 113.37, 34.17, 33.78, and 33.14 ppm. Elem. anal. Calcd for $C_{11}H_{13}Br$: C, 58.69; H, 5.82. Found: C, 58.63; H, 5.99.

Synthesis of 3-(4-Vinylphenyl)propane-1-thiol (1). Thiourea (2.5 g, 33 mmol) was added to the solution of **5** (2.0 g, 9 mmol) in methanol (100 mL), and the mixture was refluxed for 16 h in an inert atmosphere. The solution was cooled to room temperature and NaOH (10 mL, 12%) was added. The solution was refluxed for 4 h to hydrolyze the thiouronium salt. 1N H_2SO_4 was added dropwise until neutral pH. Fifty milliliters of water was added and the product was extracted with CH_2Cl_2 (3 × 50 mL). The organic phase was washed with water (2 × 50 mL) and then saturated NaCl (2 × 50 mL). The solvent was removed under a vacuum, and the product was purified by flash chromatography on silica gel using CH_2Cl_2 (R_f = 0.95 by TLC) and then semipreparative HPLC using 98% hexane and 2% ethyl acetate. The solvent was removed under vacuum to give **1** as a colorless liquid (74%). ^{1}H NMR (270 MHz, $CDCl_3$): δ 7.33 (d, 2 H, J = 7.9 Hz), 7.13 (d, 2 H, J = 7.9 Hz), 6.69 (q, 1 H), 5.75 − 5.66 (m, 1 H), 5.23−5.16 (m, 1 H), 2.71 (t, 2 H, J = 7.2 Hz), 2.52 (q, 2 H), 1.35 (t, 1 H, J = 7.9 Hz). ^{13}C NMR (67.5 MHz, $CDCl_3$): 141.07, 136.67, 135.54, 128.71, 126.36, 113.18, 35.43, 34.13, 24.01 ppm. EIMS (178 (70) [M^+], 144 (56) [$C_{11}H_{12}^+$], 117 (100) [$C_9H_9^+$]. Elem. anal. Calcd for $C_{11}H_{14}S$: C, 74.10; H, 7.91. Found: C, 74.38; H, 7.62.

Synthesis of Surface-Mounted Nanothin Films. Freshly stripped gold substrates (0.5 cm × 1.5 cm)[13] were submersed in 10 mL of 0.1% (by volume) solution of **1** in hexane in the lid of a weighing dish (15 mL capacity). These samples were then placed in a Rayonet Photochemical Chamber Reactor (Model RPR-200) that was oriented horizontally. The sample was placed on a stand within the cabinet so that it was 7 in. from two 254 nm lamps (35 W each) that were directly above the sample, so that the substrate and solution were directly exposed to the ultraviolet light. The lamps were turned on and samples (duplicate) were removed at 5, 10, 30, and 60 min. After about 30 min, a rubberlike white solid appeared in the solution. The substrates were removed from the solution and immediately rinsed with tetrahydrofuran and then water, and were finally blown dry in a stream of compressed argon. It was critical to rinse the substrates with tetrahydrofuran to remove bulk polymer particles that had adsorbed onto the surface. Subsequent deposition steps were performed as described above; the irradiation time was 30 min.

Film Thickness Measurement by Optical Ellipsometry. Film thicknesses were measured using a Stokes Ellipsometer LSE with 632.8 nm HeNe laser by Gaertner Scientific Corporation. Average values for optical parameters at 5 positions across each bare gold substrate were used for the thickness measurement model. Thickness measurements were taken at 5 positions across each substrate. 1.45 was used as the refractive index of the SAM. The monolayer kinetics were measured in a home-built fluid cell constructed from microscope with windows normal to the beam. The complex refractive index of the gold surface was measured both in air and in hexane. 1.3749 was used as the refractive index of hexane. The complex refractive index of the gold in hexane (n = 0.4394, k = −4.9191) was used as the input substrate parameter for monitoring of the film growth.

Gel Permeation Chromatography (GPC). 3 mL of 0.1% solution of **1** in hexane was polymerized in a small Petri dish as described above, and the sample was allowed to dry (30 min). To the precipitate was added 3 mL of THF. A 2 mL aliquot of the supernatant was injected into a Shimadzu Prominence GPC system. The column used was a 250 mm × 10 mm (ID) Jordi oligomer column packed with a 500 Å divinylbenzene gel. The pump was run with a THF eluent at isocratic flow at 1 mL/min. The column oven was set at 35 °C. The detector was a Shimadzu refractive index detector, model RID-10A, held at a cell temperature of 40 °C and with a response of 1.5 s.

Monitoring of the Polymerization with Gas Chromatography (GC). Toluene was used as an internal standard. A 2 μL/mL solution of toluene in hexane was prepared as a standard stock solution. A 0.1% solution of **1** was prepared with this standard as a solvent. Calibration standards were prepared by diluting the 0.1% of **1** in hexane with the standard to a concentration range of 0.01 mM to 0.1 mM. The calibration curve was prepared from seven data points over this range. Thirty milliliters of the stock solution was poured into a 100 mm × 20 mm Petri dish, set on a scale, in a Rayonet UV chamber equipped with 8 254 nm lamps positioned overhead and from the sides in a semicircle. The lamps were turned on. Before starting and every 5 min until 30 min, a 0.5 mL aliquot of this solution was extracted using an automatic pipet. At each interval, the weight of the solution remaining was measured so that the concentration calculations could compensate for the evaporation of hexane. The sample aliquots were passed through a 0.5 cm deep column of neutral aluminum oxide to remove oligomers and bulk polymer. The columns were washed with 2 mL of the standard and collected in glass vials for GC analysis. The GC experiment was carried out in a Hewlett-Packard 5890 Series II gas chromatograph equipped with a flame ionization detector set at 250 °C. Helium was used as the carrier gas and the detector gases were air and hydrogen. The column was a Valcobond capillary column (15 m × 0.25 mm × 25 m) with 100% PDMS as the stationary phase. Ten microliters of sample was injected into an injection port set at 200 °C. The oven was initially set at 70 °C, but after 1.5 min wait time, the temperature was ramped to 250 °C at 25°/min. The length of the experiment was 15 min.

Electrochemical Characterization. The insulating properties of the films were evaluated by cyclic voltammetry and impedance spectroscopy using an Autolab Potentiostat (model PGSTAT12). The substrates were fixed onto the bottom of plexiglass chambers (Ø = 6.4 mm) using an O ring fitting. The exposed area defined by the O ring was 28 mm^2 in all experiments. The chamber was filled with the test solution and an alligator clip was attached to an end of the gold coated substrate. The voltage of the working electrode (annealed template stripped (ATSG) substrates coated with nanothin film) was scanned against a Ag/AgCl/1 M KCl reference electrode (CH Instruments, Austin, TX) which was immersed into the test solution. In the cyclic voltammetric experiments 0.1 V/s scan rate was used. The nanothin film coated ATSG electrode impedances were analyzed in $K_4Fe(CN)_6$, H_2O_2, and in ferrocene methanol (FcMeOH) solutions in the frequency range between 50 mHz and 60 kHz at 10 mV amplitude. The potential between the reference and working electrode was set to 0.2, 0.6, and 0.2 V, respectively.

AFM Characterization. AFM topography and phase images were gathered using an MFP-3D instrument purchased from Asylum Research (Santa Barbara, CA) with included software. All images were collected in repulsive AC mode. The cantilevers used were AC240TS manufactured by Olympus and purchased from Asylum Research. Images were flattened using a zero-order processing algorithm included in the MFP-3D software.

Attenuated Total Reflectance (ATR)-IR Measurements. The ATR-IR measurements were carried out using a a grazing angle ATR accessory with a fixed 65° incident angle and a hemispherical Ge crystal purchased form Harrick Scientific. Spectra were recorded on a Thermo Nicolet 380 FTIR spectrometer with 2000 scans at 4 cm^{-1} resolution. Background spectrum of a freshly cleaned gold substrate was subtracted from the spectrum of the film.

Contact Angle. Contact angle measurements were performed on a ramé-hart model 200 goniometer. For each sample, five droplets of water were deposited in different places, contact angles were measured using the included software, and the results were averaged.

Results and Discussion

Compound **1** was synthesized as shown in Scheme 1. The Friedel−Crafts acylation of commercially available 3-bromopropylbenzene **2** with acetic anhydride produced the acetyl derivative **3**. The reduction of **3** with sodium borohydride formed a benzylic alcohol **4**, which was dehydrated in acidic conditions to give a styrene derivative **5**. Thiol moiety was introduced by the reaction of **5** with thiourea followed by alkaline hydrolysis. The overall isolated yield of **1** from commercially available compound **2** was 11% without optimizing conditions for the synthesis.

Scheme 1. Synthesis of 3-(4-Vinylphenyl)propane-1-thiol

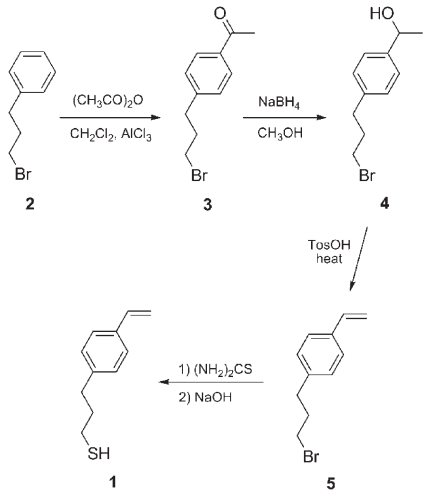

Neat **1** and its concentrated solutions gradually oligomerize upon storage as evidenced by decreased signals from vinyl hydrogens in ^{1}H NMR spectra. A dilute solution of **1** in hexane (0.1%) can be stored in a refrigerator for several months without noticeable oligomerization.

Compound **1** formed a self-assembled monolayer on the gold surface after a brief exposure of freshly cleaned gold surface to the solution of **1** in hexane (0.1% by volume). Except as noted below, we used annealed template-stripped (ATSG) gold substrates prepared by a straightforward procedure developed in our group.[13] These substrates are characterized by low (<0.5 nm) roughness and large grain size. The formation of the monolayer was observed with in situ ellipsometry.

To prepare the polymer films, gold substrates were immersed in hexane solution of **1**, and the samples were irradiated with UV light for 60 min. Within approximately 30 min, white material began to precipitate. The IR spectrum of this material was consistent with polystyrene derivative, which is expected to form because of the bulk polymerization of **1**. The material did not completely dissolve in THF, suggesting that the polymer was cross-linked. GPC analysis of the extracts from this material showed broad variations in molecular weight, mostly in the range of 400−8500. The samples were then removed from the solution and rinsed with hexane and THF to remove the polymeric material precipitated from hexane. The film growth was complete within 1 h (Figure 3A). Immediately after film deposition, gold surfaces were dried and analyzed by ellipsometry and atomic force microscopy (AFM). The film thickness was highly reproducible and uniform.

The concentration of **1** was monitored in the solution with GC. In these experiments, an aliquot of hexane solution was taken at regular intervals and analyzed on a GC using an internal standard after passing the solution through a short alumina column to remove polymers (Figure 4). The disappearance of the starting material closely followed kinetics of the film growth (Figure 3). The decrease of the starting material concentration was fit into first-order kinetics. It appears that the film stops growing because of the depletion of starting material in solution.

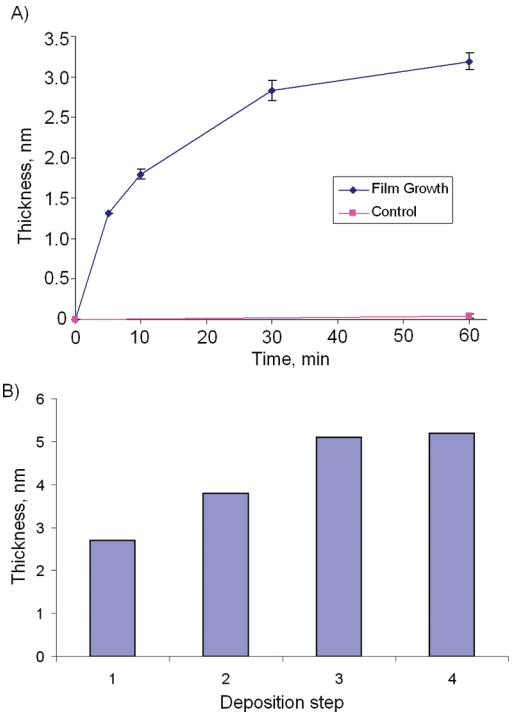

Figure 3. Controlled film growth. (A) Growth of nanothin films on gold surfaces as a function of UV irradiation exposure time. (B) Sequential depositions of nanothin film onto the same gold substrate; each deposition step consisted of 30 min of UV irradiation in fresh solution of **1** in hexane.

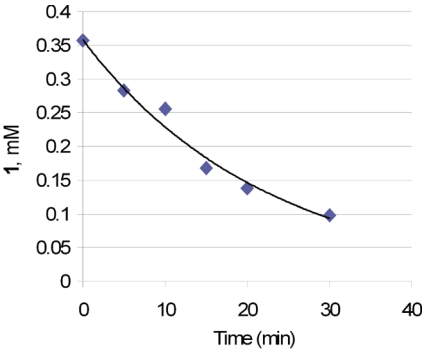

Figure 4. Disappearance of **1** monitored by GC.

We found that partially oligomerized **1** (as determined by ^{1}H NMR) is also capable of forming nanothin films. These films exhibit characteristics similar to those of the films grafted from **1**.

When a film is exposed to a fresh solution of **1**, UV irradiation causes further film growth (Figure 3B). Second and third deposition steps added approximately 1 nm each to the total film thickness. No further increase in thickness was observed when the film was exposed to fresh solutions of **1**. The smaller film growth observed during the additional polymerization steps indicates a lower amount of polymerizable functional groups on the film surface. The prospect of covalently binding material

(13) Banner, L. T.; Richter, A. G.; Pinkhassik, E. *Surf. Interface Anal.* **2009**, *41*, 49–55.

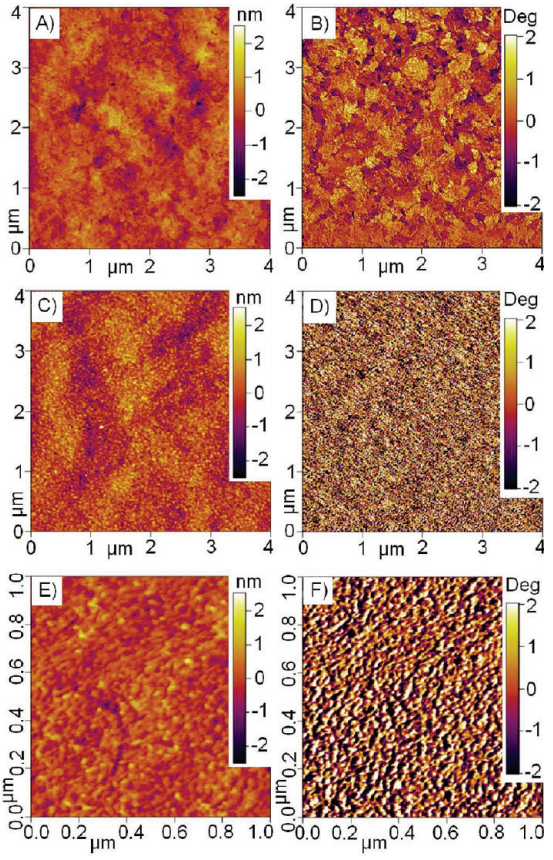

Figure 5. (A, C, E) AFM topography and (B, D, F) phase imaging shows complete surface coverage and uniform film thickness: (a) bare TSG gold substrate height (z range = 5 nm; mean roughness = 0.34 nm; rms roughness = 0.43 nm); (b) bare TSG gold substrate phase (z range = 4°); (c) 3.1 nm film on TSG gold substrate height (z range = 5 nm; mean roughness = 0.36 nm; rms roughness = 0.57 nm), roughness is similar to that of the bare gold substrate; (d) 3.1 nm film on TSG gold substrate phase (z range = 4°), polycrystalline structure of bare gold is now obscured; (e) 3.2 nm film on ATSG gold substrate height (z range = 5 nm; mean roughness = 0.32 nm; rms roughness = 0.41 nm); (f) 3.2 nm film on ATSG gold substrate phase (z range = 4°).

on top of a polymerized layer opens exciting opportunities for controlling the chemical environment of the outer layer of a film. One can envision that different functional groups can be introduced into the parent molecule **1** for binding of other molecules. Sequential deposition process offers greater flexibility in creating functional coatings, i.e., one could create a layered film structure with a uniform and robust bottom layer where a top layer with different functional groups for molecular recognition, catalysis, sensing, or even separations is extended. In addition, sequential deposition allows controlling the film thickness in a broader range.

AFM imaging provided conclusive evidence of uniform thickness and complete coverage of the gold surface (Figure 5). We used template-stripped gold (TSG) substrates for AFM imaging on Figure 5A−D to highlight the polycrystalline gold structure, clearly visible here because of the small grain size of TSG substrates. Topography scans showed that polymer films with 3 nm thickness (Figure 5C) have approximately the same roughness as bare gold (Figure 5A) confirming uniform film thickness. A phase image of bare gold shows polycrystalline structure of the gold substrate (Figure 5B). In contrast, the phase image of film-coated surface shows that the polycrystalline structure of the underlying substrate is obscured (Figure 5D). Close-up images of the nanofilm obtained with an ATSG substrate (Figure 5E,F) further confirm uniform film thickness.

The attenuated total reflectance (ATR) IR spectrum of the film is consistent with a polystyrene-based film. Bands corresponding to aromatic and aliphatic C−H (3050 − 2800 cm^{-1}) and aromatic C=C bonds (1700−1550 cm^{-1}) are conspicuous in the spectrum. However, bands corresponding to the of S−H (expected in the 2500−2600 cm^{-1} region) bonds are not visible in the IR spectrum, consistent with disappearance of most of thiol groups due to S−C bond formation, which supports participation of thiol groups in cross-linking of polystyrene chains. As expected, large number of $-CH_2-$ groups result in prominent bands corresponding to aliphatic C−H bonds (2950 − 2800 cm^{-1}). Multiple signals in the 1700−1500 cm^{-1} region indicate different environments for the aromatic moieties, consistent with the plausible structure shown in Figure 2.

Contact angle measurements are consistent with the presence of a small amount of thiol groups on the surface. We measured the water contact angle for the 3 nm film to be 80 ± 2°, which suggests that our films are slightly more hydrophilic than amorphous polystyrene (90°)[14].

The insulating properties of the film were tested by cyclic voltammetry (CV) and impedance spectroscopy. In Figure 6 we show cyclic voltammograms recorded with ATSG electrodes with one (6A), two (6B) and three (6C) layers of nanothin film coatings. The experiments were performed in a pH 7.2 phosphate buffer containing also 0.1 M KNO_3 as supporting electrolyte (a) and in solutions in which the supporting electrolyte contained also 1 mM K_4 $Fe(CN)_6$ (b), 1 mM FcMeOH (d), or 50 mM H_2O_2 (c). As can be seen in Figure 6A even a single layer of the nanothin film on the ATSG electrode surface blocks the oxidation of 50 mM H_2O_2 (small hydrophilic molecule with no charge and 50 times larger concentration as the K_4 $Fe(CN)_6$ and FcMeOH used in these experiments). Two consecutively deposited layers reduce the oxidation current of $Fe(CN)_6^{4-}$ (hydrophilic anion with high charge density and relatively large molecular weight) to about one-third of its original value (Figure 6B). Finally, three layers completely block the electrochemical oxidations of H_2O_2 and $Fe(CN)_6^{4-}$ (Figure 6C) on the ATSG electrode. However, the oxidation current remained significant on the ATSG electrode in the presence of 1 mM FcMeOH (a small hydrophobic molecule without charge) even with three layers of polymer coating (Figures 6A−C). Apparently, FcMeOH partitions into the hydrophobic film and thus it can reach the ATSG electrode surface by diffusion where it is oxidized. With the increasing film thickness, the concentration gradient between the ATSG electrode and solution sides of the nanofilm decreases,

(14) Bortolotti, M.; Brugnara, M.; Della Volpe, C.; Siboni, S. *J. Colloid Interface Sci.* **2009**, *336*, 285–297.

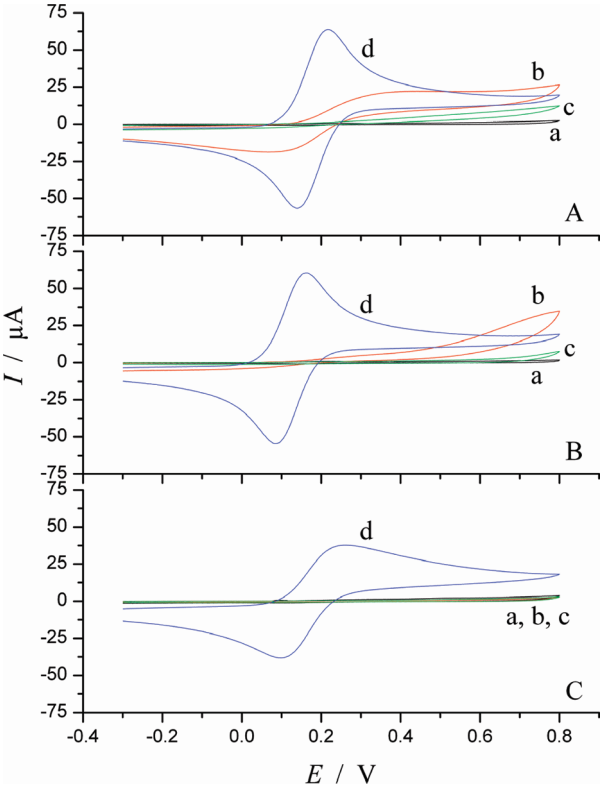

Figure 6. Cyclic voltammograms recorded with $v = 0.1$ V s^{-1} scan rate using nanothin polymeric film coated ATSG electrodes: (A) single layer, (B) two layers, and (C) three layers. The CVs were recorded in (a) supporting electrolyte solution, and in supporting electrolytes spiked with (b) 1 mM $K_4Fe(CN)_6$, (c) 50 mM H_2O_2, or (d) 1 mM ferrocene methanol (FcMeOH). As supporting electrolyte a pH 7.20 phosphate buffer (0.1 M HK_2PO_4/H_2KPO_4) with 0.1 M KNO_3 was used.

and consequently the peak current decreases. Once a film-coated electrode has been exposed to a FcMeOH-containing solution, numerous washing steps were required to remove FcMeOH residues from the film. The removal of other analytes from the nanothin film coated electrode surface, i.e., repeating the washing cycles until the current drops to its background value in the supporting electrolyte, was much simpler.

The impedance analysis of the membrane coated electrodes are in agreement with our findings in the cyclic voltammetric experiments and provided quantitative data on the electrical resistance and capacitance of the films. The impedance experiments were performed with one, two, or three layers of nanothin films deposited over the ATSG electrodes in the presence of a supporting electrolyte solution containing 1 mM $K_4Fe(CN)_6$, 1 mM FcMeOH, or 50 mM H_2O_2. In all three electrolytes, the film impedances increased gradually upon the deposition of multiple layers; however, the absolute values of the measured impedances were different. In agreement with our expectations based on the CVs shown in Figure 6, the largest impedances were recorded in the presence of H_2O_2, whereas the smallest in the presence of FcMeOH as electroactive species. In Figure 7, we show the impedance plots (imaginary impedance Z'' vs the real impedance Z') recorded in a background electrolyte containing 1 mM $K_4Fe(CN)_6$.

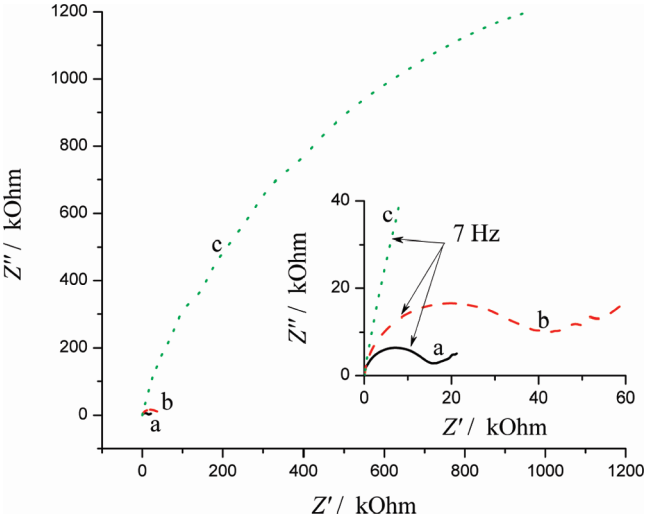

Figure 7. Impedance spectra of ATSG electrodes covered with (a) one, (b) two, and (c) three layers of nanothin polymeric films. Electrolyte: 1 mM $K_4Fe(CN)_6$ in 0.1 M KNO_3 + 0.1 M HK_2PO_4/H_2KPO_4 (pH 7.2) supporting electrolyte; frequency range between 50 mHz and 60 kHz; amplitude, 10 mV; applied potential, $E = 0.2$ V. Inset: Impedance plot at higher magnification in a limited impedance range.

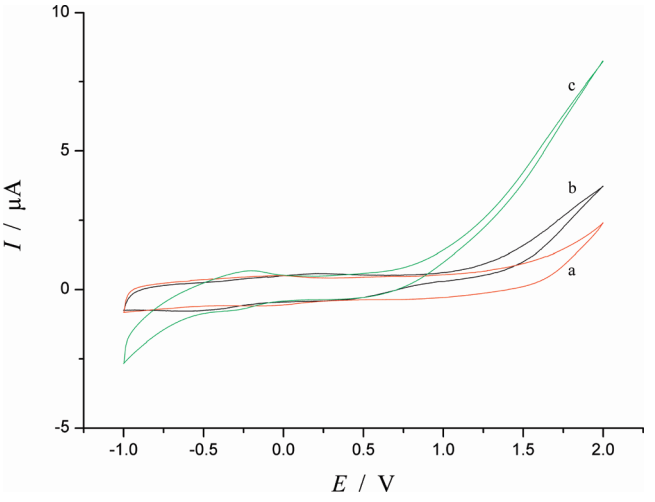

Figure 8. Cyclic voltammograms of ATSG electrodes covered with 3 layers of polymer films after scanning the electrode potential between −1 V and +2 V 50 cycles in presence of (a) 0.5 M H_2SO_4, (b) 0.1 M KNO_3, 0.01 M HK_2PO_4/H_2KPO_4 (pH 7), and (c) in the same supporting electrolyte as in b but also containing 1 mM $K_4Fe(CN)_6$. Scan rate: 0.1 V s^{-1}.

To test the stability, robustness, and insulating properties of the surface bound nanothin films of this study in comparison to "conventional" SAMs, we scanned the potential of ATSG electrodes with three layers of nanothin film coatings between −1 V and +2 V for 50 cycles. Cycling the potential of a working electrodes in such wide potential range is commonly used to strip a SAM from its surface, e.g., dodecanethiol.[15] We were also interested in the suppression of the gold oxide formation and the oxide stripping currents by the surface- grafted nanothin film.[16] Figure 8 shows CVs recorded with the ATSG electrode

(15) Campiña, J. M.; Martins, A.; Silva, F. *Electrochim. Acta* **2008**, *53*, 7681–7689.
(16) Finklea, H. 0.; Avery, S.; Lynch, M. *Langmuir* **1987**, *3*, 409–413.

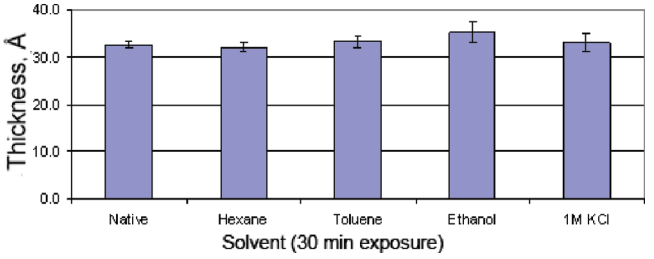

Figure 9. Freshly synthesized surface-mounted nanothin film on gold substrate was submersed in 5 mL of hexane, toluene, ethanol, and 1 M KCl for 30 min each. After each submersion the substrates were removed from the solution and were immediately washed with water and then blown dry in a stream of compressed argon. The thickness of the film was then measured by ellipsometry.

with three layers of nanothin film coatings in air saturated 0.5 M H_2SO_4, a pH 7.20 phosphate buffer containing also 0.1 M KNO_3 and in the same buffer containing also 1 mM $K_4Fe(CN)_6$. The recorded traces show no indication of gold oxide formation or oxide stripping. Apparently, the three-layer coating not only blocked the oxidation of hexacyanoferrate(II) ions, but also prevented the oxidation of the gold surface at potentials higher than 0.7 V. In agreement with our AFM data, the results suggest that the hydrophobic film is free from pinholes and protects the gold surface from water and/or oxygen molecules. Remarkably, successive cycling of the electrode potential made the film more resistive. The current measured at 2 V decreased to approximately 50% of its original value after 50 cycles. We assume that the increase in the film resistance for the duration of cycling the electrode potentials in this very broad potential range is due to an increase in the level of cross-linking in the film and/or the electrochemical oxidation of monomer residues or precursor molecules in the film. Apparently, this process is pH dependent.

The films were also remarkably stable toward prolonged treatment with hexane, toluene, ethanol, and 1 M KCl, rapid flux of water, and vigorous mechanical agitation. In these experiments, ellipsometry measurements showed no change in film thickness after exposure to the above conditions (Figure 9).

Good stability and chemical resistance are essential for practical applications of thin films. To illustrate robustness of new films, we coated a copper penny with the nanofilm following the same protocol as for coating gold substrates. Coated samples were placed in household bleach (approximately 5% NaOCl in water) for 24 h along with control samples that were not coated. Coated

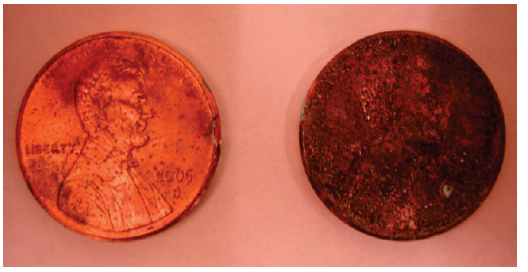

Figure 10. Coated (left) and uncoated (right) pennies after 24 h exposure to 5% NaOCl solution.

samples were well-preserved, whereas uncoated samples showed significant corrosion (Figure 10).

Conclusions

In summary, we demonstrated controlled formation of robust nanometer-thin films from a newly synthesized compound **1** that combines a styrene moiety and a thiol group joined by a short linker. The thiol group binds the film to the surface and enables its growth by cross-linking polystyrene chains. Films can be deposited in layers, which opens opportunities for creating multilayer films with programmed functionality. The films are uniform in thickness and provide a complete surface coverage with no noticeable pinholes. Films are insulating and stable under a broad range of conditions, making them suitable for a variety of applications. One can envision using molecular imprinting to create pores for use in electrochemical sensors or as docking sites in molecular electronics. The film deposition begins with a well-established SAM technology. The possibility of combining SAM patterning techniques such as dip-pen nanolithography[17] (e.g., patterning **1**, masking the rest of the surface, and building up a robust patterned film) with our robust film fabrication further enhance these films' utility.

Acknowledgment. This work was supported by a National Science Foundation CAREER Award (CHE-0349315), National Institutes of Health grant (1R01HL079147-01) and a FedEx Institute of Technology Innovation Award.

Supporting Information Available: Detailed spectral and chromatographic characterization and contact angle measurements.This material is available free of charge via the Internet at http://pubs.acs.org.

(17) Salaita, K.; Wang, Y. H.; Mirkin, C. A. *Nat. Nanotechnol.* **2007**, *2*, 145–155.